Tetrahedron 67 (2011) 8102–8109

Contents lists available at SciVerse ScienceDirect

Tetrahedron

journal homepage: www.elsevier.com/locate/tet

Fluoride-induced intermolecular excimer formation of bispyrenyl thioureas linked by polyethylene glycol chains

Duangrat Thongkum, Thawatchai Tuntulani *

Supramolecular Chemistry Research Unit, Department of Chemistry, Faculty of Science, Chulalongkorn University, Bangkok 10330, Thailand

ARTICLE INFO

Article history:
Received 10 April 2011
Received in revised form 27 July 2011
Accepted 22 August 2011
Available online 27 August 2011

Keywords:
Pyrene
π–π Stacking
Hydrogen bonding
Intermolecular excimer formation
Fluoride probe

ABSTRACT

New bispyrenyl thioureas linked by polyethylene glycol (PEG) chains, **L1**–**L3**, and methoxy benzene pyrene thiourea, **L4**, were synthesized. Upon binding with F^- in $CHCl_3$, **L1**–**L3** exhibited strong excimer emission bands (I_E) and weak monomer emission bands (I_M), while **L4** displayed the same intensity of both bands. However, little or no change was observed in fluorescence spectra of **L1** upon adding OH^-, AcO^-, BzO^-, $H_2PO_4^-$, Cl^-, Br^-, and I^-. Therefore, only F^- induced the pyrene excimer formation. Job's plots showed 1/1 or 2/2 complexation of **L1** with F^-. Ratios of I_E/I_M of **L1**·F^- complex were dependent on the concentration of **L1**, implying that the dimerization of **L1** proceeded via the intermolecular excimer formation. Among **L1**–**L4**, **L1** possessed the highest binding constant and sensitivity toward F^- implying the importance of the linking PEG chain. **L1** was demonstrated to be an excellent probe for F^- in $CHCl_3$ with the detection limit as low as 46.2 μg/L.

1. Introduction

Fluoride plays an important role in human life, and the deficiency or overexposure of the amount of fluoride causes osteoporosis and poor dental health.[1] Many synthetic sensors for detection of fluoride have been reported via various sensing mechanisms, such as fluoride sensing by covalent bonding with cationic borane,[2] by hydrogen-bonding with thioureas,[3] by fluoride-π interactions,[4] and by fluoride-induced tautomerism of sensors.[5] Accordingly, there is still a need to develop a highly sensitive and selective sensor for fluoride using new and simple mechanisms. We are interested in the design and synthesis of receptors for sensing fluoride where the recognition occurred through various mechanisms in only one receptor: (i) hydrogen-bonding, (ii) π–π stacking, and (iii) conformational change of a flexible link.

Pyrene is a polycyclic aromatic hydrocarbon consisting of four fused benzene rings, resulting in a flat aromatic system. The number of π-electrons in pyrene can be increased by the intramolecular or intermolecular overlapping of p-orbitals with the π-conjugated system. Therefore, pyrene and its derivatives have often been used as dyes and fluorescence probes because of their high sensitivity for detection via excimer formation.[6] Bispyrenyl compounds containing two pyrene units linked by a short flexible alkyl chain were found to give high local concentration of chromophores in solutions, and this resulted in the enhancement of emission signals.[7] We hypothesized that if we linked two thiourea-modified pyrene units with a flexible chain of polyethylene glycol or PEG, an inert polymer composed of repeating units of CH_2CH_2O,[8] we should obtain an anion sensor that can give an emission of the pyrene excimer band resulting from stacking of two pyrenes upon binding anions.

Herein, we reported the synthesis of compounds **L1**–**L3** containing various chain lengths of PEG linking with pyrene thioureas at both ends, and a control pyrene thiourea **L4** without the PEG chain (Fig. 1). The synthesized molecules were examined for their abilities to form π–π stacking interactions upon binding anions, especially fluoride, using NMR spectroscopy and spectrofluorometry.

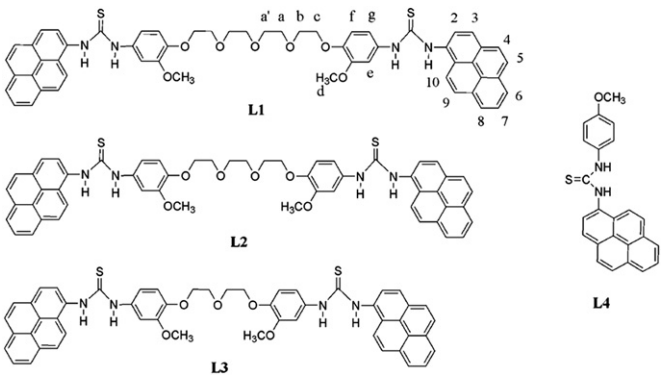

Fig. 1. Structures of **L1**–**L4**.

* Corresponding author. Tel.: +66 2 2187643; fax: +66 2 2187598; e-mail address: thawatchai.t@chula.ac.th (T. Tuntulani).

0040-4020/$ – see front matter © 2011 Elsevier Ltd. All rights reserved.
doi:10.1016/j.tet.2011.08.060

2. Results and discussion

2.1. Synthesis and photophysical properties of L1–L4

Compounds **L1**–**L3** containing various chain lengths of PEG and pyrene thioureas at both ends were synthesized by the procedure shown in Scheme 1. Compound **1**, 2-methoxyphenol, underwent a nitration reaction using concentrated HNO_3/CH_3COOH in CH_3CN to give compound **2** in 16% yield. Substitution reaction of **2** with an appropriate polyethylene glycol ditosylate in the presence of K_2CO_3 in CH_3CN resulted in compounds **3**, **4**, and **5** in 76%, 55%, and 63% yields, respectively. Reduction of **3**, **4**, and **5** with Raney Ni and hydrazine gave **6**, **7**, and **8**, respectively, in quantitative yields. Coupling reactions between **6**, **7**, and **8** and compound **9**, 1-isothiocyanatopyrene, in $CHCl_3$ at room temperature gave **L1**, **L2**, and **L3** in 48%, 38%, and 52% yields, respectively. The control compound, **L4**, was synthesized to compare the anion binding ability in the absence of PEG. Compound **10** underwent a methylation reaction with CH_3I in the presence of K_2CO_3 in CH_3CN to give compound **11** in 95% yield. Compound **11** was then reduced using Raney Ni and hydrazine to give compound **12** in a quantitative yield. The coupling reaction between **12** and **9** in $CHCl_3$ gave **L4** in 32% yield. All synthesized compounds were well soluble in nonpolar organic solvents, such as dichloromethane, chloroform and in polar organic solvents, such as DMSO. ^{1}H NMR and ^{13}C NMR spectroscopy, mass spectrometry, and elemental analysis were used to confirm the structures of ligands **L1**–**L4** (Fig. S1–S8 in Supplementary data).

UV–vis absorption spectra of compounds **L1**–**L4** were studied in $CHCl_3$ solution exhibiting two major absorption bands for the $\pi-\pi^*$ transition of aromatic hydrocarbons in the range 250–400 nm (Fig. S9 in Supplementary data). These bands represent the characteristic shape of the pyrene group for $S_0 \rightarrow S_1$ and $S_0 \rightarrow S_2$ transitions.[9] Fluorescence emission spectra of **L1**–**L4** in $CHCl_3$ displayed only intense characteristic monomer bands of pyrene between 390 and 410 nm (Fig. S10 in Supplementary data). Upon increasing concentrations of **L1**–**L4** to 10^{-4} M, no excimer bands were observed. The fluorescence emissions of **L1**–**L3** were observed in almost the same intensity at the concentration as low as 5×10^{-6} M. However, the emission spectrum of **L4** showed a very weak monomer band at this concentration. Therefore, the emission of **L4** was measured at 5×10^{-5} M. The fluorescence quantum yields of all synthesized receptors were calculated using the integrated emission intensity of anthracene as a standard.[10] The absorption and emission parameters for compounds **L1**–**L4** in $CHCl_3$ are summarized in Table 1. It should be noted that the quantum yields increased upon increasing the chain lengths of PEG.

Table 1
The absorption and emission parameters for compounds **L1**–**L4** in $CHCl_3$

Compound	Absorption		Emission	
	λ_{abs} (nm)	$\varepsilon\times10^4$ (L mol^{-1} cm^{-1})	λ_{em} (nm)	Φ_F[a] (%)
L1	347	6.58	402	19
L2	347	6.60	407	12
L3	347	6.29	401	11
L4	346	3.04	393	6

[a] Fluorescence quantum yields used anthracence as a standard (Φ_{ST}=0.27 in EtOH).

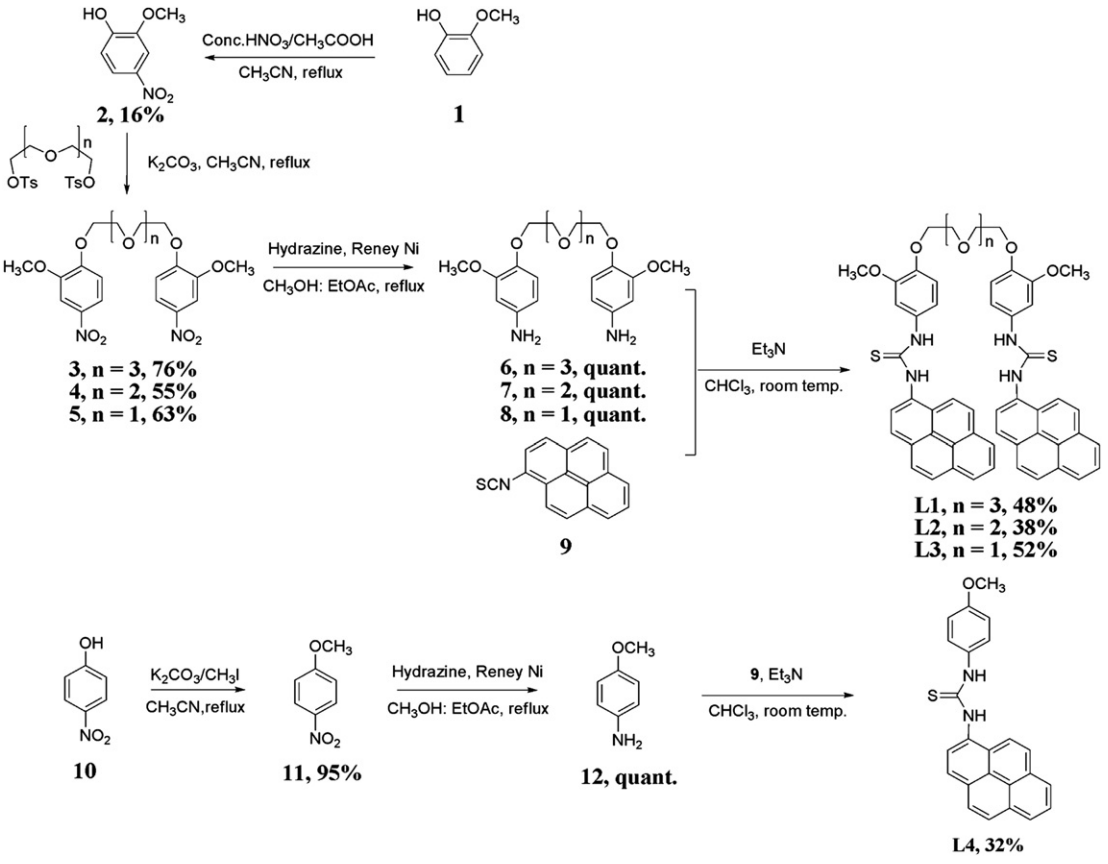

Scheme 1. Synthetic procedure for **L1**–**L4**.

2.2. Anion binding studies

The anion binding properties of **L1** toward tetrabutylammonium (TBA) salts of anions were investigated in $CHCl_3$ solution using spectrofluorometry. Upon adding 100 equiv of F^-, OH^-, AcO^-, BzO^-, $H_2PO_4^-$, Br^-, Cl^-, and I^- into a solution of **L1** (5.0×10^{-6} M), only the fluorescence spectrum of **L1**·F^- displayed a pyrene excimer band at 500 nm when excited at 340 nm (Fig. 2). Little or no change was observed in the fluorescence spectra of **L1** in the presence of other anions. Therefore, only F^- can induce the excimer formation of pyrene in $CHCl_3$.

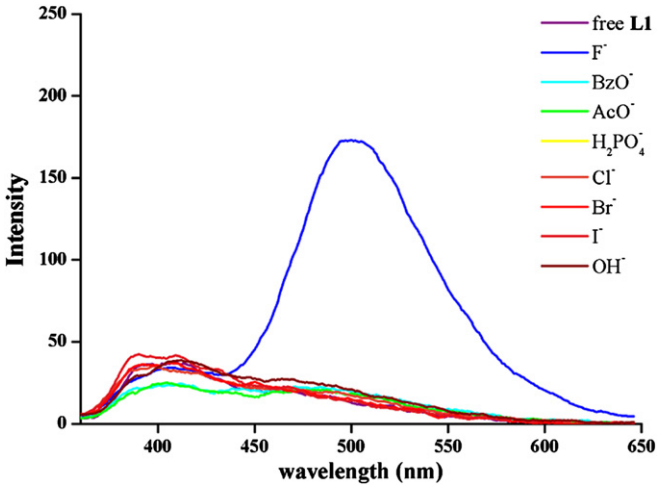

Fig. 2. Fluorescence emission of **L1** (5.0×10^{-6} M) with 100 equiv TBA anion salts in $CHCl_3$.

Excimers are dimers in the excited state. This term results from the contraction of excited dimer. The pyrene excimer formed by the π–π stacking between two pyrene molecules. The fluorescence band corresponding to an excimer is located at higher wavelength than that of monomer and does not show vibronic bands. Two important informations from an emission spectrum are fluorescence intensity ratio of excimer to monomer emission (I_E/I_M) and maximum wavelength of excimer emission (λ_E). This ratio is sensitive to the structure change while the λ_E is much less variable and is usually located at 475–500 nm.[6]

The order of intensity ratio between excimer and monomer bands (I_E/I_M) of **L1** in the presence of anions varied as $F^->AcO^-\approx BzO^->H_2PO_4^-\approx Cl^->Br^-\approx I^->OH^-$ (Fig. 3). The

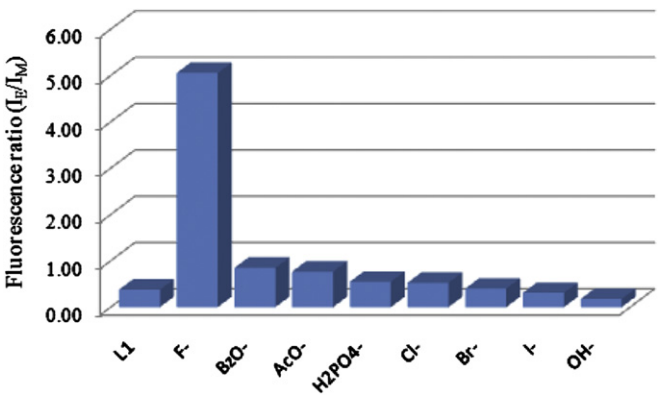

Fig. 3. Plot of the intensity ratio of excimer to monomer emission (I_E: 500 nm, I_M: 400 nm) of **L1** (5.0×10^{-6} M) with 100 equiv. TBA anion salts in $CHCl_3$.

preference of fluoride to bind with –NH of thiourea groups through H-bond was due to its higher basicity. Moreover, the smallest atomic size of fluoride was suitable to encapsulate in the receptor molecule. Interestingly, the complexation of **L1** with OH^- displayed the minimum I_E/I_M ratio, even the OH^- possessed the highest basicity. This suggested that not only the basicity of anions but also the size of anions was an important factor that affected the binding ability of **L1**.

The fluorescence titration spectra of **L1** with fluoride (Fig. 4) displayed the fluorescence intensity enhancement of pyrene excimer band at 500 nm, which gradually increased until the addition of fluoride anions into **L1** solution reached 100 equiv. However, there was a small change in monomer emission intensity at 398 nm. These suggested that the fluoride induced the formation of π–π stacking of pyrene resulting in the enhancement of the excimer band. From the fluorescence titration data, the binding constants (K_s) for the formation of **L1** with each anion were calculated via Benesi–Hildebrand plots,[9] and the ratio of the interception at the origin to the slope yielded K_s. The binding constant of **L1**·F^- was found to be higher than that of $H_2PO_4^-$, BzO^-, and AcO^- as shown in Table 2. Therefore, **L1** was selective toward fluoride. This result agreed with previous results reported by Gozen in which the unfolded structure of pseudocyclic tristhiourea showed a common preference for $F^->H_2PO_4^->AcO^-$.[11]

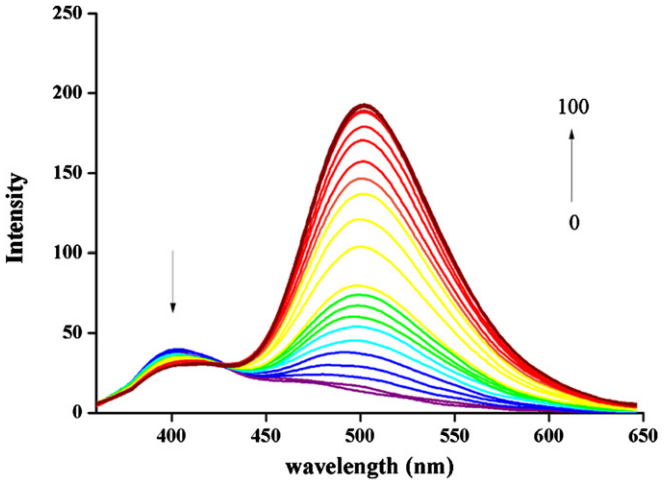

Fig. 4. Fluorescence titration spectrum of **L1** (5.0×10^{-6} M) with TBAF (0–100 equiv) in $CHCl_3$.

Table 2
Binding constant (M^{-1}) of receptor **L1** and TBA anion salts in $CHCl_3$

L1·anion	K_s	R^2	Ratio	$\lambda_{ex}/\lambda_{em}$
F^-	1.0×10^4	0.9969	1/1	340/500
BzO^-	5.8×10^3	0.9918	1/1	340/408
AcO^-	4.2×10^3	0.9936	1/1	340/398
$H_2PO_4^-$	7.5×10^3	0.9991	1/1	340/391
Cl^-	NA	NA	NA	340/412
Br^-	NA	NA	NA	340/404
I^-	NA	NA	NA	340/407
OH^-	NA	NA	NA	340/400

NA=values cannot be determined.

The Job's plot of **L1** with fluoride displayed a maximum complexation at the mole fraction of 0.5 suggesting 1/1 or 2/2 complexation of **L1** with fluoride (Fig. S11 in Supplementary data). Therefore, a possible structure of the **L1**·F^- complex could be a folded structure from the intramolecular pyrene–pyrene stacking

or an unfolded structure of the intermolecular pyrene–pyrene stacking as shown in Fig. 5.

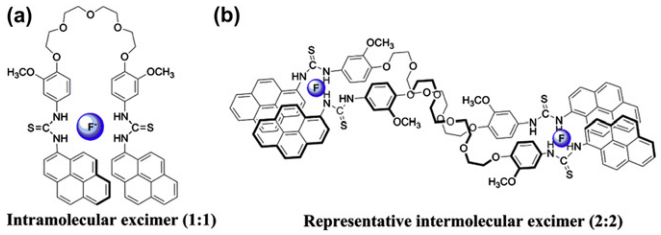

Fig. 5. The possible structures of **L1**·F^- complex.

Besides **L1**, the anion binding properties of **L2**–**L4** with fluoride were also studied by spectrofluorometry (Figs. S12–S14 in Supplementary data). The fluorescence titration profiles of **L2**·F^- and **L3**·F^- complexes displayed the excimer band emerged obviously compared to the monomer band in the same manner as **L1**·F^- complex. However, in the case of **L4**·F^-, both excimer and monomer bands showed similar fluorescence intensity. The binding constants of **L1**, **L2**, **L3**, and **L4** toward F^- can be calculated by Benesi–Hildebrand plots,[9] and are found to be 1.0×10^4, 1.0×10^3, 6.3×10^3, and 5.4×10^2 M^{-1} for **L1**, **L2**, **L3**, and **L4**, respectively. Therefore, **L1** is the most efficient probe for detecting fluoride because a longer flexible PEG chain may reduce the repulsion between the methoxy group and the oxygen of PEG to provide a more stable pyrene-stacking complex. In addition, F^- is the smallest anion and provides the least steric hindrance guests for binding with **L1**.

The role of the PEG linkage on the sensitivity of **L1** and **L4** toward fluoride was investigated by monitoring the fluoride induced an excimer emission at the minimum ligand concentrations in $CHCl_3$. In the presence of 100 equiv of fluoride, the minimum concentrations of **L1** and **L4** for detection of the excimer emission band were 5×10^{-6} M and 5×10^{-5} M in $CHCl_3$, respectively. The fluorescence intensity at 500 nm of **L1**·F^- is two times as high as the fluorescence intensity of **L4**·F^-, even at lower concentration (Fig. 6). Therefore, the excellent sensitivity of **L1** and weaker sensitivity of **L4** indicated that the PEG linkage on **L1** significantly improves sensitivity and binding ability of **L1** toward F^-.

2.3. π–π Stacking formation of pyrenes induced by fluoride: effects of solvents and metal ions

^1H NMR spectra of **L1** and **L1** in the presence of 4 equiv of F^-, AcO^-, BzO^-, and $H_2PO_4^-$ in $CDCl_3$ are illustrated in Fig. 7. Generally, the benzene protons (H_e, H_f, and H_g) of all spectra displayed downfield shifts because of the inductive effect from anions. All the PEG protons (H_a, H_b, and H_c) and the methoxy protons (H_d) were almost unchanged indicating that the PEG chain and methoxy oxygen did not involve in anion binding. Interestingly, signals of pyrene protons of the complexes shifted downfield in the presence of AcO^-, BzO^-, and $H_2PO_4^-$ due to inductive effects from the anions. However, in the case of F^- the signal of pyrene protons became broader and some protons shifted more upfield as compared to pyrene signals in other spectra. The broadening and shielding of these signals stemmed from the anisotropic effect of the stacking-pyrene ring current induced by F^-.[12,13] This ring current caused some pyrene protons inside an anisotropic region to be deshielded and other pyrene protons outside the anisotropic region to be shielded. This NMR spectrum supported that F^- induced π–π stacking of the pyrene rings in the complex of **L1**·F^-.

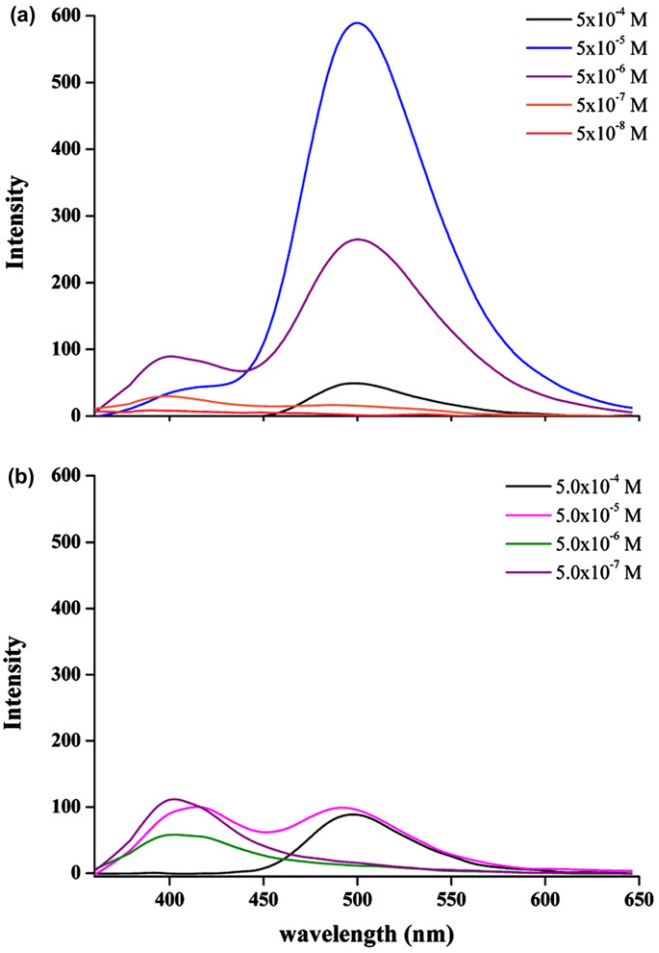

Fig. 6. Fluorescence emission spectra of various concentrations of (a) **L1** and (b) **L4** with 100 equiv of TBAF in $CHCl_3$.

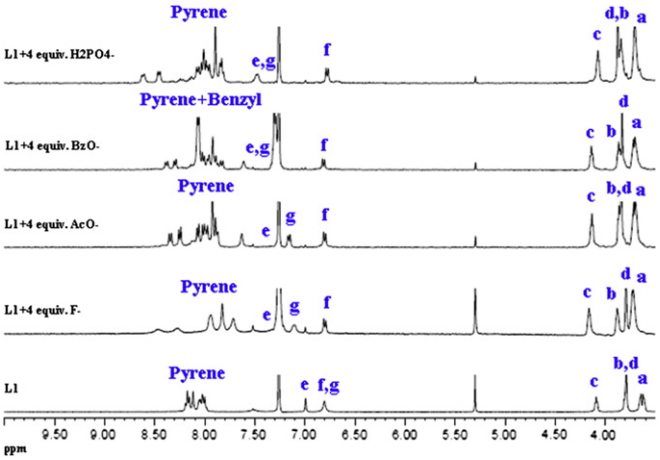

Fig. 7. ^1H NMR spectra of **L1** in the presence of 4 equiv of tetrabutylammonium F^-, AcO^-, BzO^-, and $H_2PO_4^-$ in $CDCl_3$ at 400 MHz.

Unfortunately, the protons of thiourea groups were overlapped with the pyrene protons when $CDCl_3$ was used as a solvent. Therefore, we could not follow a shift of the NH protons, which participated in hydrogen bonding interactions with fluoride. When using DMSO-d_6 as a solvent, NH signals were observed in the NMR spectrum (Fig. S1 in Supplementary data), but disappeared completely upon addition of 4 equiv of fluoride probably due to the deprotonation of the NH proton by F^-.[14]

In addition, NOESY of **L1**·F^- in $CDCl_3$ was carried out to assign the correlation between protons in the space. The NOESY connection of the PEG protons and the benzene protons was clearly observed only for the signal of adjacent protons, H_a and H_b, H_b and H_c, H_c and H_f as well as H_f and H_g. Therefore, these protons were in the same space (Fig. S15 in Supplementary data).[15] Unfortunately, the signal of pyrene protons could not be assigned clearly due to overlapping of the complicated proton signal. Therefore, this technique cannot be used to differentiate clearly between the intramolecular and intermolecular excimer formation.

Either intramolecular or intermolecular interactions can be observed in a molecule with two reactive groups connected by a flexible link.[16] The intramolecular formation between these reactive molecules produces a macrocyclic ring-closure product, and the intermolecular formation results in a dimer and oligomer structures. The I_E/I_M ratios of the former are independent of substrate concentrations, while the latter are not. Therefore, in normal solutions where diffusion is rapid, high substrate concentrations favor polymerization while cyclizations occur in good chemical yields only at low concentrations.[17]

In order to elucidate whether the pyrene stacking of **L1** induced by fluoride occurred in the intramolecular or intermolecular fashion, the ratios of I_E/I_M of **L1** in the presence of 100 equiv of F^- in various concentrations were monitored. Fig. 8 shows that the fluorescence intensity ratios of excimer and monomer depended on the concentration of ligand, which gradually decreased in the concentration range of 5.0×10^{-4} M to 5.0×10^{-8} M. These results suggested the pyrene stacking of **L1**·F^- complex proceeded via the intermolecular manner in which the representative structure was shown in Fig. 5b.[17] The intermolecular excimer structure of **L1** did not need to fold the podand chain to bind fluoride and could reduce the steric hindrance on the receptor molecule. Therefore, the intermolecular excimer structure (Fig. 5b) should be more thermodynamically favorable than the intramolecular excimer structure (Fig. 5a).

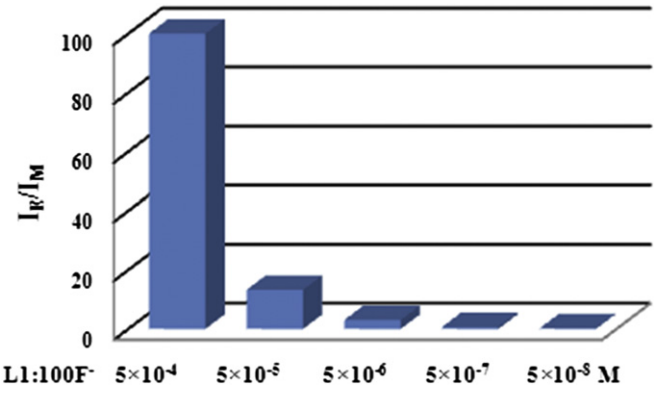

Fig. 8. Plot of I_E/I_M of TBAF (100 equiv) with various concentration of **L1**.

Interestingly, our results agreed with the intermolecular pyrene stacking in bichromophoric pyrene azine induced by Hg^{2+} reported by Martinez et al.[6c] Upon addition of Hg^{2+} to the mentioned ligand, there was a small change in monomer emission intensity and a strong increase in excimer emission, similar to the addition of F^- to the solution of **L1**.

L1 contains a podand chain from the PEG linkage, which is able to form complexes with alkali metal ions,[16] the fluorescence titration of **L1** with alkali metal, such as sodium or potassium has been carried out and exhibited no excimer bands (Fig. S16 in Supplementary data). ^1H NMR spectra of **L1** in the presence of alkali metal ions in $CDCl_3/CD_3CN$ (9/1 v/v) showed small shifts in the methylene region and almost unchanged in the aromatic region. Therefore, the π–π stacking interactions between two pyrene units could not be induced by the alkali metals. Moreover, upon addition of sodium or potassium to the $CDCl_3/CD_3CN$ (9/1 v/v) solution of **L1**+4 equiv of F^- resulted in the original spectrum of **L1**. This indicated decomplexation of **L1**·F^- occurred in the presence of Na^+ or K^+ (Fig. S17 in Supplementary data). This behavior was similarly found in the fluorescence titration. The excimer emission intensity at 500 nm of **L1**+100 equiv of F^- was gradually quenched by adding aliquots of sodium perchlorate (Fig. S18 in Supplementary data). These experiments suggest that the π–π interactions induced by fluoride are very weak and can be destroyed by ion-pairing.

It has been established that solvents can affect π–π interactions[18] and can, therefore, perturb the pyrene excimer formation. Our studies found that the fluorescence spectra of **L1**·F^- showed the intensity enhancement of the excimer band upon increasing the percentage of hexane in chloroform solution (Fig. S19 in Supplementary data). However, the excimer band intensity decreased upon adding 5% of methanol in chloroform solution of **L1**·F^-. Therefore, both metal ions and polar protic solvents can disrupt the intermolecular π–π stacking interactions of pyrene.

2.4. Use of the synthesized compounds as fluoride sensors

To test the efficiency of all synthesized ligands for sensing fluoride, the ratios of excimer to monomer intensity (I_E/I_M) were compared between **L1** and **L4** with each anion and with mixed anions as shown in Fig. 9. The I_E/I_M ratios of **L1**–**L3** in the presence of AcO^-, BzO^-, $H_2PO_4^-$, Cl^-, Br^-, and I^- showed very low emission ratio as compared to that in the presence of F^-. From the last column in Fig. 9, it can be concluded that other anions can interfere with the detection of fluoride anion for all the synthesized ligands by reducing the emission ratios (I_E/I_M). However, **L1**–**L3** in anion mixtures still retain the emission ratio in a similar manner to the emission ratios found in the presence of only F^- suggesting the good selectivity for this anion, and **L1** shows the best sensing response to F^-. In the case of **L4**, the emission ratio showed insignificant difference from other columns suggesting the poor selectivity of **L4** toward F^-.

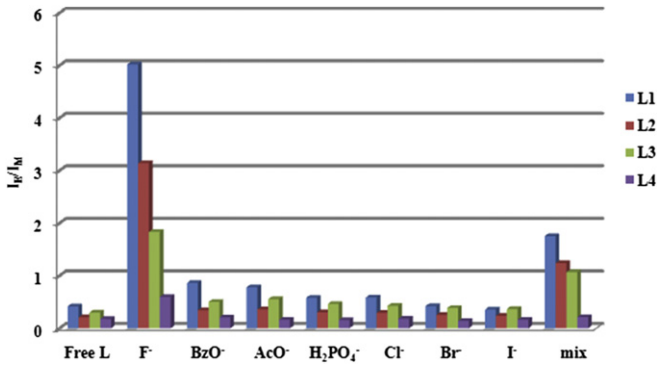

Fig. 9. Selectivity of all the synthesized ligands toward various anions (100 equiv) and the mixture of all anions.

To apply compound **L1** as a molecular sensor for F^- in $CHCl_3$, the sensing ability of **L1** toward fluoride was studied. The detection limit was calculated by using three times the standard deviation (3SD) of the background noise to estimate the lowest concentration of fluoride that can be measured from the ratio between 3SD of the fluorescence intensity at 500 nm of free **L1** and slope of the linear

plot of fluorescence titration data of **L1** with fluoride shown in Fig. 10.[19] The detection limit of **L1** (5×10^{-6} M) toward F^- was found to be 2.43×10^{-6} M or 46.2 μg/L in $CHCl_3$. The fluoride sensing response can even be detected with a naked eye for this concentration of fluoride by the appearance of the light blue fluorescence of the pyrene chromophore upon exposure to UV irradiation at 365 nm (Fig. 10, inset).

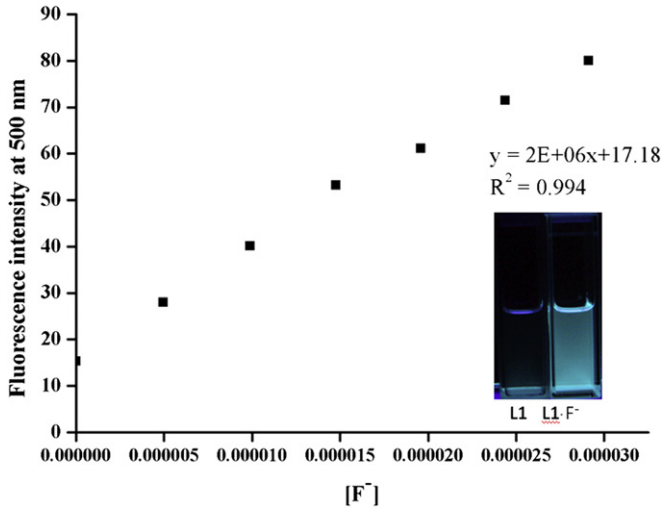

Fig. 10. The linear plot of fluorescence titration data of **L1** with F^- and fluorescence appearance of **L1** (5.0×10^{-6} M) in the presence of 46.2 μg/L of F^-.

3. Conclusion

We have synthesized new bisthiourea pyrenyl compounds linked by various PEG chains, **L1**–**L3** and the monomeric pyrene thiourea, **L4** with no PEG chain. ^{1}H NMR spectroscopy and spectrofluorometry showed that only F^- could induce the excimer formation from intermolecular pyrene stacking. The results also revealed the importance role of the PEG chain in F^- binding and sensing abilities. **L1** possessing the longest podand chain showed the best binding ability and sensitivity toward F^- while **L4** showed the worst sensing and binding ability. Therefore, **L1** could be an excellent sensor for F^-. It was demonstrated to detect as low as 46.2 μg/L of F^- in $CHCl_3$.

4. Experimental

4.1. General

^{1}H NMR and ^{13}C NMR spectra were recorded with a Varian Mercury Plus 400 NMR spectrometer and a Bruker Ultrashield™ Plus 400 NMR spectrometer. 2D NOESY spectrum was recorded on Varian Mercury Plus 400 NMR spectrometer. Fluorescence spectra were recorded on a Varian Cary Eclipse fluorescence spectrophotometer. UV–vis spectra were recorded on a Varian Cary 50 UV–vis spectrometer.

All compounds were synthesized under nitrogen atmosphere. Compounds **1**, 2-methoxyphenol, and **10**, 4-nitrophenol, were obtained from Merck and Aldrich, respectively. PEG ditosylates were synthesized from PEGs and *p*-toluenesulfonyl chloride by adapting methods from the previously published procedure.[20] Compound **9**, 1-isothiocyanatopyrene, was synthesized using the procedure reported previously.[21] All materials and reagents were standard analytical grade, and used without further purification. Commercial grade solvents, methanol, dichloromethane, hexane, ethylacetate, were distilled before use. The progress of the reactions was monitored by TLC on silica gel and visualized by UV light. The chromatographic separations were performed on silica gel columns (0.063–0.200 mm) to purify the synthesized compounds.

DMSO-d_6 and $CDCl_3$ were used as solvents for NMR experiments. In complexation studies, anions were used in their tetrabutylammonium salts. The binding constants between the ligand and various ions were determined by the linear equation of Benesi–Hildebrand plots.

4.2. Syntheses of L1–L4

*4.2.1. Compound **2**.* The mixture of **1** (2.12 g, 0.017 mol) in CH_3CN (30 mL) and CH_3COOH (15 mL) was stirred under nitrogen. A solution of concentrated HNO_3 1.20 mL in 15 mL of CH_3CN was then added dropwise and refluxed. The reaction was stirred at room temperature for 12 h. After that, the reaction was cooled to 0 °C, and the pH was adjusted to 7–8 by saturated HCO_3^- solution. The solvent was removed by a rotary evaporator. The resulting residue was extracted with CH_2Cl_2 and water. The organic phase was isolated and dried over anhydrous Na_2SO_4. The solvent was removed, and the crude was purified by column chromatography with CH_2Cl_2 as eluent. The product was collected and recrystallized with hexane/CH_2Cl_2 to give compound **2** as yellow solid (0.45 g, 16%). Mp: 121.0–122.0 °C. MALDI-TOF (*m*/*z*) $[M]^+$: calcd 169.04, found 170.93. IR (KBr): 1510 ($\nu_{asym.\ NO2}$), 1341 ($\nu_{sym.\ NO2}$) cm^{-1}. ^{1}H NMR (400 MHz, $CDCl_3$) δ 7.88 (dd, *J*=8.8, 2.4 Hz, 1H), 7.76 (d, *J*=2.4 Hz, 1H), 6.98 (d, *J*=8.8 Hz, 1H), 6.43 (s, 1H), 3.99 (s, 3H) ppm. ^{13}C NMR (100 MHz, $CDCl_3$) δ 151.7, 146.1, 141.2, 118.6, 114.0, 106.4, 56.5 ppm.

*4.2.2. Compounds **3**–**5**.* Generally, the mixture of a polyethylene glycol, compound **2**, K_2CO_3, and tetrabutylammonium bromide in CH_3CN (50 mL) was stirred and refluxed under nitrogen. After 2 days, the solvent was removed and pH of the mixture was adjusted to 1 with 3 M HCl. The residue was extracted with CH_2Cl_2 (25×3 mL) and H_2O. The organic phase was collected and dried over anhydrous Na_2SO_4. The solvent was removed, and the product was recrystallized with CH_3OH to yield compounds **3**–**5**.

Compound **3** was obtained as a yellow solid (0.27 g, 76%). Mp: 114.0–116.0 °C. MALDI-TOF (*m*/*z*) $[M]^+$: calcd 496.17, found 496.56. IR (KBr): 1518 ($\nu_{asym.\ NO2}$), 1338 ($\nu_{sym.\ NO2}$) cm^{-1}. ^{1}H NMR (400 MHz, $CDCl_3$) δ 7.86 (d, *J*=8.4 Hz, 2H), 7.71 (s, 2H), 6.94 (d, *J*=8.8 Hz, 2H), 4.26 (s, 4H), 3.92 (s, 10H), 3.72 (s, 4H), 3.66 (s, 4H) ppm. ^{13}C NMR (100 MHz, $CDCl_3$) δ 153.8, 149.0, 141.5, 117.6, 111.3, 106.6, 70.9, 70.6, 69.3, 68.7, 56.2 ppm.

Compound **4** was obtained as a yellow solid (0.16 g, 55%). MALDI-TOF (*m*/*z*) $[M]^+$: calcd 452.14, found 452.65. IR (KBr): 1518 ($\nu_{asym.\ NO2}$), 1346 ($\nu_{sym.\ NO2}$) cm^{-1}. ^{1}H NMR (400 MHz, $CDCl_3$) δ 7.87 (dd, *J*=8.8, 2.8 Hz, 2H), 7.73 (d, *J*=2.8 Hz, 2H), 6.94 (d, *J*=8.8 Hz, 2H), 4.27 (t, *J*=4.8, 5.2 Hz 4H), 3.93 (t, *J*=5.2, 4.4 Hz, 10H), 3.75 (s, 4H) ppm. ^{13}C NMR (100 MHz, $CDCl_3$) δ 153.9, 149.2, 141.7, 117.6, 111.4, 106.8, 71.0, 69.4, 68.9, 56.3 ppm.

Compound **5** was obtained as a yellow solid (0.14 g, 63%). MALDI-TOF (*m*/*z*) $[M]^+$: calcd 408.12, found 408.73. IR (KBr): 1508 ($\nu_{asym.\ NO2}$), 1339 ($\nu_{sym.\ NO2}$) cm^{-1}. ^{1}H NMR (400 MHz, $CDCl_3$) δ 7.87 (dd, *J*=8.8, 2.8 Hz, 2H), 7.73 (d, *J*=2.8 Hz, 2H), 6.94 (d, *J*=8.8 Hz, 2H), 4.30 (t, *J*=4.4, 5.2 Hz, 4H), 4.01 (t, *J*=4.4, 4.8 Hz, 4H) 3.93 (s, 6H) ppm. ^{13}C NMR (100 MHz, $CDCl_3$) δ 153.7, 149.1, 141.6, 117.5, 111.3, 106.6, 69.6, 68.8, 56.2 ppm.

*4.2.3. Compounds **6**–**8**.* A mixture of **3**–**5** (0.201 mmol) in CH_3OH (5 mL) and EtOAc (10 mL) was stirred with molecular sieve under nitrogen. After 15 min, Raney Ni (1/4 spoon) and 2 mL of hydrazine hydrate were added and refluxed for 1 h. The color of the reaction was changed from yellow to colorless solution. The

molecular sieve and Raney Ni were removed by filtration. The residue was evaporated to dryness and extracted with CH_2Cl_2 and H_2O. The organic phase was collected and dried over anhydrous Na_2SO_4. Solvent was evaporated to give a yellow oil product in a quantitative yield. The product was used in the next step without further purification.

*4.2.4. Compound **11**.* A mixture of **10** (3.48 g, 0.025 mol), anhydrous K_2CO_3 (1.73 g, 0.0125 mol) in CH_3CN (25 mL) was refluxed under nitrogen. CH_3I (3 mL, 0.0482 mol) in CH_3CN (25 mL) was added dropwise to the mixture. After 5 h, the solvent was removed under reduced pressure. The residue was dissolved in CH_2Cl_2 and 3 M HCl was added until the pH of the solution became 1. The solvent was removed, and the resulting residue was extracted with CH_2Cl_2 (25 mL×3) and water. The organic phase was dried over anhydrous Na_2SO_4, filtered, and the solvent was removed. The crude residue was purified by column chromatograph using CH_2Cl_2 as eluent to yield compound **11** as a yellowish green solid (3.65 g, 95%). MALDI-TOF (m/z) $[M]^+$: calcd 153.04, found 153.99. IR (KBr): 1500 ($\nu_{asym.\ NO2}$), 1333 ($\nu_{sym.\ NO2}$) cm^{-1}. ^1H NMR (400 MHz, $CDCl_3$) δ 8.19 (dd, J=7.2, 2.0 Hz, 2H), 6.95 (dd, J=7.2, 2.0 Hz, 2H), 3.9 (s, 3H) ppm. ^{13}C NMR (100 MHz, $CDCl_3$) δ 164.6, 141.6, 125.9, 114.0, 56.0 ppm.

*4.2.5. Compound **12**.* A mixture of **11** (0.05 g, 0.3 mmol) in CH_3OH (1 mL) and EtOAc (20 mL) was stirred with molecular sieve under nitrogen. After 15 min, Raney Ni (1/4 spoon) and 2 mL of hydrazine hydrate were added and refluxed for 1 h. The color of the reaction was changed from yellow to colorless. The molecular sieve and Raney Ni were removed by filtration. The residue was evaporated to dryness and extracted with CH_2Cl_2 and H_2O. The organic phase was collected and dried over anhydrous Na_2SO_4. Solvent was evaporated to give a yellow oil. The product was used in the next step without purification.

*4.2.6. Compound **L1**.* A solution of compound **6** (0.100 mmol) and triethylamine (0.10 mL, 0.717 mmol) in $CHCl_3$ (10 mL) was stirred under nitrogen at room temperature for 30 min and then compound **9** (0.066 g, 0.255 mmol) in $CHCl_3$ (20 mL) was added to the reaction. The reaction mixture was stirred for 3 days and then evaporated to dryness. The residue was extracted with CH_2Cl_2 and H_2O. The organic phase was collected and evaporated to dryness and purified by column chromatography using EtOAc as eluent. The final product **L1** was recrystallized with CH_2Cl_2/CH_3OH to give a yellow solid (0.046 g, 48%). Mp: 140.0–142.8 °C. MALDI-TOF (m/z) $[M^+]$: calcd 954.31, found 953.0. Elemental analysis for $C_{56}H_{50}N_4O_7S_2$: calcd C, 70.42; H, 5.28; N, 5.87. Found C, 70.40; H, 5.23; N, 5.82. IR (KBr): 1513 ($\nu_{C=S}$) cm^{-1}. ^1H NMR (400 MHz, $CDCl_3$) δ 8.0 (m, 22H), 7.0 (s, 2H), 6.8 (s, 4H), 4.1 (s, 4H), 3.8 (s, 10H), 3.6 (d, J=7.6 Hz, 8H) ppm. ^{13}C NMR (100 MHz, DMSO-d_6) δ 181.2, 148.5, 145.3, 133.2, 132.6, 130.6, 130.4, 129.2, 127.3, 127.1, 127.0, 126.7, 126.4, 126.3, 125.3, 125.1, 124.8, 124.4, 123.8, 122.7, 116.7, 113.0, 109.7, 69.8, 69.7, 68.9, 68.0, 55.4 ppm.

*4.2.7. Compound **L2**.* A similar procedure to the preparation of **L1**, **L2** was synthesized from the coupling reaction of compound **7** and compound **9**. The compound **L2** was obtained as yellow powders (0.035 g, 38%). MALDI-TOF (m/z) $[M]^+$: calcd 910.290, found 909.407. Elemental analysis for $C_{54}H_{46}N_4O_6S_2$: calcd C, 71.19; H, 5.09; N, 6.15. Found C, 71.05; H, 4.92; N, 6.20. IR (KBr): 1509 ($\nu_{C=S}$) cm^{-1}. ^1H NMR (400 MHz, DMSO-d_6) δ 10.07 (s, 2H), 9.73 (s, 2H), 8.31–8.06 (m, 18H), 7.20 (d, J=2 Hz, 2H), 6.97 (dd, J=27, 8.8 Hz, 4H), 4.04 (t, J=4.8 Hz, 4H), 3.74 (m, 10H), 3.60 (s, 4H) ppm. ^{13}C NMR (100 MHz, DMSO-d_6) δ 181.2, 148.5, 145.3, 133.2, 132.6, 130.6, 130.4, 129.2, 127.3, 127.2, 127.0, 126.7, 126.4, 126.4, 125.3, 125.1, 124.9, 124.4, 123.8, 122.7, 116.8, 113.0, 109.7, 69.9, 68.9, 68.0, 55.4 ppm.

*4.2.8. Compound **L3**.* A similar procedure to the preparation of **L1**, **L3** was synthesized from the coupling reaction of compound **8** and compound **9**. The compound **L3** was obtained as yellow powders (0.045 g, 52%). MALDI-TOF (m/z) $[M]^+$: calcd 866.26, found 865.07. Elemental analysis for $C_{52}H_{42}N_4O_5S_2$: calcd C, 72.03; H, 4.88; N, 6.46. Found C, 72.25; H, 4.86; N, 6.42. IR (KBr): 1509 ($\nu_{C=S}$) cm^{-1}. ^1H NMR (400 MHz, DMSO-d_6) δ 10.02 (s, 2H), 9.69 (s, 2H), 8.28–8.02 (m, 18H), 7.16 (d, J=2 Hz, 2H), 6.92 (m, 4H), 4.03 (t, J=4 Hz, 4H), 3.71 (m, 10H) ppm. ^{13}C NMR (100 MHz, DMSO-d_6) δ 181.0, 148.4, 145.1, 133.0, 132.5, 130.4, 130.2, 129.0, 127.2, 127.0, 126.8, 126.5, 126.3, 126.2, 125.1, 124.9, 124.7, 124.2, 123.6, 122.5, 116.6, 113.0, 109.5, 68.8, 67.9, 55.2 ppm.

*4.2.9. Compound **L4**.* Compound **12** (0.300 mmol) and triethylamine (0.20 mL, 1.5 mmol) in $CHCl_3$ (10 mL) was stirred under nitrogen at room temperature for 30 min and then compound **9** (0.093 g, 0.360 mmol) in $CHCl_3$ (20 mL) was added to the reaction. The reaction mixture was stirred for 3 days, and the solvent was evaporated to dryness. The residue was extracted with CH_2Cl_2 and H_2O. The organic phase was collected, evaporated to dryness, and purified by recrystallization with CH_2Cl_2/EtOAc to give a white solid of **L4** (0.037 g, 32%). MALDI-TOF (m/z) $[M]^+$: calcd 382.11, found 382.70. Elemental analysis: for $C_{24}H_{18}N_2OS$: calcd C, 75.37; H, 4.74; N, 7.32. Found C, 75.40; H, 4.83; N, 7.41. IR (KBr): 1512 ($\nu_{C=S}$) cm^{-1}. ^1H NMR (400 MHz, $CDCl_3$) δ 8.05 (m, 11H), 7.32 (d, J=8 Hz, 2H), 6.90 (d, J=8 Hz, 2H), 3.79 (s, 3H) ppm. ^{13}C NMR (100 MHz, DMSO-d_6) 181.6, 156.6, 133.0, 132.2, 130.6, 130.4, 129.2, 127.3, 127.1, 126.9, 126.6, 126.4, 126.3, 125.3, 125.1, 124.8, 124.4, 123.8, 122.6, 113.5, 55.1 ppm.

4.3. Spectrofluorometry

4.3.1. Anion titrations. Solutions of compounds **L1**–**L3** (5.0×10^{-6} M) and **L4** (5.0×10^{-5} M) were prepared in a 10 mL volumetric flask and 2 mL of each ligand was pipetted into a 1 cm path length quartz cuvette. The emission spectra were recorded in the range 360–650 nm at room temperature by using the excitation wavelength at 340 nm. The solution of an anion (1.0×10^{-3} or 1.0×10^{-2} M up to concentration of ligand) was prepared in a 10 mL volumetric flask and transferred to a 2 mL microburette. The anion solution was introduced in portions to the cuvette and stirred for 60 s prior to measurement.

4.3.2. Metal ion titrations. The preparations of the ligands were similar to the titration of anions. However, the sodium solution (1.0×10^{-3} M or 1.0×10^{-2} M) was prepared in CH_3CN and was introduced in portions to the cuvette by a microburette. The mixture between the ligand and sodium was stirred for 2 min prior to measurement.

4.4. ^1H NMR spectroscopy

4.4.1. Anion titrations. The solution of a ligand (1.0×10^{-3} M) in $CDCl_3$ (0.5 mL) was prepared in a 5 mm of an NMR tube. The ^1H NMR spectrum of the free ligand was recorded. The solution of fluoride ion (1.0×10^{-2} M) in $CDCl_3$ (1.0 mL) was prepared in a vial. Then, fluoride solution was added in portions to the NMR tube via a microsyringe (10 and 50 μL portions). ^1H NMR spectrum of the mixture was recorded.

4.4.2. Metal ion titrations. The solution of ligand **L1** (1.0×10^{-3} M) in $CDCl_3/CD_3CN$ (9/1 v/v) (0.5 mL) was prepared in a 5 mm NMR tube. The ^1H NMR spectrum of free ligand was recorded. The solution of

sodium ion (1.0×10^{-2} M) in $CDCl_3/CD_3CN$ (1.0 mL) was prepared in a vial and was added via a microsyringe to the free ligand solution. ^1H NMR spectra were recorded after each addition.

4.5. Anion interferences

Fluorescence spectra of compound **L1** (5.0×10^{-6} M, 2 mL) were measured in the presence of F^-, AcO^-, BzO^-, $H_2PO_4^-$, Cl^-, Br^-, and I^- (8.5×10^{-3} M, 0.12 mL of each anion). Then, the emission spectrum of compound **L1** was recorded in the presence of mixed anions.

4.6. Detection limit of L1

The fluorescence intensity of **L1** (5.0×10^{-6} M) at 500 nm was recorded 10 times to find the standard deviation. The fluorescence titrations of **L1** (5.0×10^{-6} M) with F^- (1.0×10^{-3} M) were carried out and the emission intensity at 500 nm was recorded. The detection limit of **L1** with F^- was calculated from the ratio between three times standard deviation of fluorescence intensity of **L1** and the slope of the fluorescence titration data of **L1** with F^-.

Acknowledgements

We would like to thank Commission on Higher Education for supporting the grant to D.T. to pursue her Ph.D. under the program of Strategic Scholarships for Frontier Research Network. The Thailand Research Fund (RTA5380003) and the National Research University of CHE and the Ratchadaphiseksomphot Endowment Fund (AM1006A) are acknowledged for financial support.

Supplementary data

^1H and ^{13}C NMR spectra of **L1**–**L4**; UV–vis spectra of **L1**–**L4**; NOESY of **L1** with TBAF; ^1H NMR and fluorescence titration spectra of **L1**–**L4** with various ions. Supplementary data associated with this article can be found, in the online version, at doi:10.1016/j.tet.2011.08.060.

References and notes

1. (a) Gunnlaugsson, T.; Glynn, M.; Tocci (née Hussey), G. M.; Kruger, P. E.; Pfeffer, F. M. *Coord. Chem. Rev.* **2006**, *250*, 3094–3117; (b) Batista, R. M. F.; Oliveir, E.; Costa, S. P. G.; Lodeiro, C.; Raposo, M. M. M. *Org. Lett.* **2007**, *9*, 3201–3204; (c) Yeo, H. M.; Ryu, B. J.; Nam, K. C. *Org. Lett.* **2008**, *10*, 2931–2934; (d) Kumar, M.; Kumar, R.; Bhalla, V. *Tetrahedron* **2009**, *65*, 4340–4344; (e) Upadhyay, K. K.; Mishra, R. K.; Kumar, V.; Chowdhury, P. K. R. *Talanta* **2010**, *82*, 312–318.
2. (a) Lee, M. H.; Gabbaı, F. P. *Inorg. Chem.* **2007**, *46*, 8132–8138; (b) Kim, Y.; Gabbaı, F. P. *J. Am. Chem. Soc.* **2009**, *131*, 3363–3369.
3. Han, F.; Bao, Y.; Yang, Z.; Fyles, T. M.; Zhao, J.; Peng, X.; Fan, J.; Wu, Y.; Sun, S. *Chem.—Eur. J.* **2007**, *13*, 2880–2892.
4. Guha, S.; Saha, S. *J. Am. Chem. Soc.* **2010**, *132*, 17674–17677.
5. Shao, J.; Yu, X.; Lin, H.; Lin, H. *J. Mol. Recognit.* **2008**, *21*, 425–430.
6. (a) Nakahara, Y.; Matsumi, Y.; Zhang, W.; Kida, T.; Nakatsuji, Y.; Ikeda, I. *Org. Lett.* **2002**, *4*, 2641–2644; (b) Koskela, S. J. M.; Fyles, T. M.; James, T. D. *Chem. Commun.* **2005**, 945–947; (c) Martínez, R.; Espinosa, A.; Tárraga, A.; Molina, P. *Org. Lett.* **2005**, *7*, 5869–5872; (d) Abe, A. M. M.; Helaja, J.; Koskinen, A. M. P. *Org. Lett.* **2006**, *8*, 4537–4540; (e) Kim, H. J.; Kim, S. K.; Lee, J. Y.; Kim, J. S. *J. Org. Chem.* **2006**, *71*, 6611–6614; (f) Jung, H. S.; Park, M.; Han, D. Y.; Kim, E.; Lee, C.; Ham, S.; Kim, J. S. *Org. Lett.* **2009**, *11*, 3378–3381; (g) Romero, T.; Caballero, A.; Tárraga, A.; Molina, P. *Org. Lett.* **2009**, *11*, 3466–3469; (h) Hung, H. C.; Cheng, C. W.; Ho, I. T.; Chung, W. S. *Tetrahedron Lett.* **2009**, *50*, 302–305; (i) Zhou, Y.; Zhu, C. Y.; Gao, X. S.; You, X. Y.; Yao, C. *Org. Lett.* **2010**, *12*, 2566–2569.
7. Winnik, F. M. *Chem. Rev.* **1993**, *93*, 587–614 and references therein.
8. (a) Han, D.; Försterling, F. H.; Li, X.; Deschamps, J. R.; Cao, H.; Cook, J. M. *Bioorg. Med. Chem. Lett.* **2004**, *14*, 1465–1469; (b) Rocha, A.; Marques, M. M. B.; Lodeiro, C. *Tetrahedron Lett.* **2009**, *50*, 4930–4933; (c) Leblond, J.; Gao, H.; Petitjean, A.; Leroux, J. C. *J. Am. Chem. Soc.* **2010**, *132*, 8544–8545; (d) Xue, Y.; O'Mara, M. L.; Surawski, P. P. T.; Trau, M.; Mark, A. E. *Langmuir* **2011**, *27*, 296–303.
9. Valeur, B. *Molecular Fluorescence Principles and Applications*; Wiley-Vch: New York, NY, 2001.
10. Melhuish, W. H. *J. Phys. Chem.* **1961**, *65*, 229–235.
11. Dahan, A.; Ashkenazi, T.; Kuznetsov, V.; Makievski, S.; Drug, E.; Fadeev, L.; Bramson, M.; Schokoroy, S.; Kemelmakher, E. R.; Gozin, M. *J. Org. Chem.* **2007**, *72*, 2289–2296.
12. Arunkumar, E.; Chithra, P.; Ajayaghosh, A. *J. Am. Chem. Soc.* **2004**, *126*, 6590–6598.
13. (a) Umemoto, T.; Satani, S.; Sakata, Y.; Misumi, S. *Tetrahedron Lett.* **1975**, 3159–3162; (b) Klod, S.; Kleinpeter, E. *J. Chem. Soc., Perkin Trans. II* **2001**, 1893–1898; (c) Nandy, R.; Subramoni, M.; Varghese, B.; Sankararaman, S. *J. Org. Chem.* **2007**, *72*, 938–944; (d) Kumar, N. S. S.; Gujrati, M. D.; Wilson, J. N. *Chem. Commun.* **2010**, 5464–5466.
14. There are numerous examples on the deprotonation of the NH proton by F^- and other anions reported by Gunnlaugsson, Gale, and Fabbrizzi which can be found in their recent review articles. (a) Duke, R. M.; Veale, E. B.; Pfeffer, F. M.; Kruger, P. E.; Gunnlaugsson, T. *Chem. Soc. Rev.* **2010**, *39*, 3936–3953; (b) Gale, P. A. *Acc. Chem. Res.* **2006**, *39*, 465–475; (c) Amendola, V.; Esteban-Gómez, D.; Fabbrizzi, L.; Licchelli, M. *Acc. Chem. Res.* **2006**, *39*, 343–353.
15. Xu, Y. X.; Wang, G. T.; Zhao, X.; Jiang, X. K.; Li, Z. T. *J. Org. Chem.* **2009**, *74*, 7267–7273.
16. Arunkumar, E.; Ajayaghosh, A.; Daub, J. *J. Am. Chem. Soc.* **2005**, *127*, 3156–3164.
17. (a) Tung, C. H.; Yuan, Z. Y.; Wu, L. Z. *J. Org. Chem.* **1999**, *64*, 5156–5161; (b) Wu, X. L.; Luo, L.; Lei, L.; Liao, G. H.; Wu, L. Z.; Tung, C. H. *J. Org. Chem.* **2008**, *73*, 491–494.
18. Hunter, C. A.; Sanders, J. K. M. *J. Am. Chem. Soc.* **1990**, *112*, 5525–5534.
19. Ingle, J. D., Jr.; Wilson, R. L. *Anal. Chem.* **1976**, *48*, 1641–1642.
20. Tomapatanaget, B.; Pulpoka, P.; Tuntulani, T. *Chem. Lett.* **1998**, 1037–1038.
21. Sirikulkajorn, A.; Duanglaor, P.; Ruangpornvisuti, V.; Tomapatanaget, B.; Tuntulani, T. *Supramol. Chem.* **2009**, *21*, 486–494.